COMMUNICATIONS IN SCIENCE AND TECHNOLOGY
Homepage: cst.kipmi.or.id

Removal of Cr(VI) from aqueous solution by biochar derived from rice husk

Risfidian Mohadi[a], Neza Rahayu Palapa[b], Tarmizi Taher[c,d], Patimah Mega Syah Bahar Nur Siregar[c], Normah[c], Novie Juleanti[c], Alfan Wijaya[c], Aldes Lesbani[b,c,*]

[a]*Department of Chemistry, Faculty of Mathematics and Natural Sciences, Universitas Sriwijaya, Palembang 30139, Indonesia*

[b]*Graduate School, Faculty of Mathematics and Natural Sciences, Universitas Sriwijaya, Palembang 30139, Indonesia*

[c]*Research Center of Inorganic Materials and Complexes, Faculty of Mathematics and Natural Sciences, Universitas Sriwijaya, Palembang 30139, Indonesia*

[d]*Department of Environmental Engineering, Institut Teknologi Sumatera, Lampung Selatan 35365, Indonesia*

Article history:
Received: 11 February 2021 / Received in revised form: 30 April 2021 / Accepted: 7 May 2021

Abstract

In this research, biochar was produced from local paddy rice husk in Sumatera and used as a bio-sorbent of Cr(VI) in an aqueous solution. The rice husk biochar (BC) was characterized using X-ray diffraction (XRD), Fourier Transform Infra-Red (FTIR), surface area-specific, and SEM morphology analysis. This XRD characterization showed a 002 reflection at 23° with broad intense diffraction, as well as the appearance of silicate oxide, and carbon vibrations. The surface area and SEM morphologies confirm that after pyrolysis the rice husk surface contained various particle sizes with a seven-fold increase in surface area. Furthermore, the Fourier Transform Infra-Red spectra verify the presence of functional groups, such as carboxylic C=O and aromatic C=C stretching. The result of the adsorption indicated the BC follows 2nd-order reaction with a 0.004 mg/min rate constant and Langmuir isotherm models with a coefficient correlation close to unity. Also, the maximum adsorption capacity of this substance increased from 68.996 mg/g to 161.290 mg/g. The thermodynamic analysis showed a positive enthalpy and entropy value, indicating Cr(VI) adsorption is endothermic. In addition, high amounts of heat favor the adsorption process due to the decrease in Gibbs energies caused by increasing temperature. The reusability adsorption study of Cr(VI) showed BC was a good potential adsorbent in the removal of the heavy metal from an aqueous solution.

Keywords: rice husk; biochar; reusable adsorbent; Cr(VI); adsorption

1. Introduction

Chromium (Cr) is a great electroplating source and a heavy metal pollutant obtained from several industrial processes that can affect the environment [1,2]. This compound is also released from mines, pottery, and photography [3,4], with the ion structure usually formed as $^{3+}$ and $^{6+}$ in an aqueous environment. Cr Hexavalent is a rare metal ion usually obtained as chromate (CrO_4^-) and di-chromate (Cr_2O_7), with extreme toxicity dependent on its valance [4,5]. Furthermore, to protect the environment during the extraction of Cr (VI), certain treatments have been used to remove the wastewater dye, including reduction, ionic exchange, extraction, and adsorption [5–7]. Adsorption is a popular treatment that has low preparation cost, high efficiency, and is easy to operate depending on the adsorbent ability [8–10]. Research on the potential adsorbent which is inexpensive, non-toxic, and easy to prepare have been the focus of the last decade. The most appealing forms are agricultural wastes-based biomass, such as wheat straw, *mangifera indica*, bagasse, rose waste, and maize corncob [11–14].

Several research on the use of agricultural wastes as adsorbent such as the adsorption processes of s*uccinylated cellulosic* biomass using Cu(II) and Zn(II) in wastewater have been reported by Singha *et al* [11]. These processes obtained an adsorption capacity of 7.27 and 5.711 mg/g for these compounds, respectively. The research by Nadeem *et al* [12] used *mangifera indica* to adsorb these compounds from an aqueous solution, where equilibrium was reached after 120 min with adsorption capacity of 8.65 and 9.45 mg/g, respectively. Also, Iqbal *et al* [13] studied a rose waste biomass (*Rosa damascena*) to remove Cr(III) and Cr(VI) and discovered the adsorption capacity of these compounds to be 15 and 7.6 mg/g, respectively. Garg et al [15] also reported Cr(VI) adsorption using sugarcane bagasse, maize corncob, and Jatropha oil cake. The results showed that the adsorption capacities were 5.75, 3.00, and 11.75 mg/g, respectively.

According to previous research, the adsorption capacity obtained from agricultural waste biomass is still low and has limitations. Therefore, there is a growing need to find new, economical, easily available, and effective adsorbents for practical application. The natural-based and carbon-rich materials such as biochar (BC) [16,17] are used because they are effective and renewable. Present research explore BC adsorbents such as wheat [18], coconut shell [19], wheat straw [20], peat husk [21], sawdust [22], and rice husk. Furthermore, rice husk has difficulty in bio-decomposition due to its hard surface and high silicon content and mainly contains cellulose, lignin, and silicon [23]. This substance is

* Corresponding author.
Email: aldeslesbani@pps.unsri.ac.id
https://doi.org/10.21924/cst.6.1.2021.293

one of the wide agricultural by-products seen in Indonesia [24] which is thrown as a non-used waste hence polluting the environment and irrigation water [25]. Therefore, to enhance the utilization of this substance as an adsorbent, some further treatments were required [26]. BC from rice husk can be applied as an economical-potential adsorbent for the removal of heavy metal cations and organic contaminants from wastewater because it is a porous material with a large surface area that contains a rich functional group on the active sites [27,28].

Several research have used BC to adsorb heavy metals [29] including the use of rice husk biochar to adsorb Pb(II) from wastewater with an adsorption capacity of 143 mg/g as reported by Sun *et al*. Cuong *et al* [30] reported the absorbance of Cu(II) using this material at pH 5 and obtained an adsorption capacity 165 mg/g. The use of chestnut shell biochar was reported by Özcimen and Ersoy-Mericboyu [31], where the adsorption of Cu(II) in an aqueous solution reached equilibrium after 120 min and obtained an adsorption capacity of 98 mg/g. The main objective of this research was to investigate and evaluate the effectiveness of BC derived from rice husk for heavy metal removal in an aqueous solution. Also, the physical, chemical, morphological, and adsorption ability of RH and BC were investigated. The adsorption was conducted with kinetic, thermodynamic, isotherm adsorption parameters and reusability of adsorbent.

2. Materials and Methods

2.1 Preparation of BC

RH was obtained from local field paddy after washing and drying in the sun. According to Poo et al, the BC was prepared from RH by pyrolysis at 600 ^{o}C for 3 hours [32]. Subsequently, the reactor was cooled down and the substance was washed several times with water and dried at 110 ^{o}C for 48 hours.

2.2 Chemicals and instrumentations

Water was purified by Purite® ion exchange method supplied by Research Center of Inorganic Materials and Complexes, in Sriwijaya University. These chemicals were purchased from Merck and Sigma-Aldich with >99% purity and directly used without further purification. The analysis of these materials was performed by XRD powder, FTIR spectroscopy, BET surface area, thermal, and SEM image analyses. The powder XRD analysis was performed by Rigaku Miniflex-600 and the sample scanned at 1^{o}/min. Furthermore, identification of functional groups was conducted by FTIR Shimadzu Prestige-21 using KBr pellet while the BET surface area analysis was conducted using Quantachrome Micromeritic 2020 instrument and the sample degassed by liquid N_2 before the process. Also, thermal and SEM analyses were conducted by TG-DTA Shimadzu analyzer using N_2 flow and the SEM Quanta 650 Oxford instrument, respectively. The analysis of chromium was performed by UV-Visible spectrophotometer Bio-Base BK-UV 1800 PC after complexation by diphenylcarbazide as a ligand. Furthermore, the resulting complex molecule was analyzed at 543 nm.

2.3 Reusability of BC

The adsorbent was desorbed after Cr(VI) adsorption by an ultrasonic system at 30 minutes and was dried at 110 ^{o}C for 5 hours. This process was conducted by a reused adsorbent, where the reusability process was performed after five cycles of the re-adsorption process. The adsorbent stability was evaluated at the end of the re-adsorption process and the reusability procedures were repeated three times.

2.4 Adsorption of Cr(VI) by BC and RH

The effect of initial Cr(VI) concentration, temperature, and time on the Cr(VI) adsorption by BC and RH was studied. These experiments were conducted in an initial pH range of 2 to 4 because the precipitation of heavy metal ions could occur and interfere with the adsorption process measurements at pH levels higher than 4 [33]. The data obtained from the initial Cr(VI) concentration of 10, 20, 30, 40, and 50 mg/L at 303-333 K was then calculated to obtain the thermodynamic and kinetic parameters. In addition, adsorption time was conducted at 10, 20, 30, 40, 50, 60, 70, 90, 120, 150, 180, and 210 minutes. Furthermore, the thermodynamic data were obtained using Langmuir and Freundlich isotherms and also ΔG, ΔH, and ΔS [34–36] while the kinetic data were obtained by1st and 2nd order as well as Elovich kinetic models [37–39].

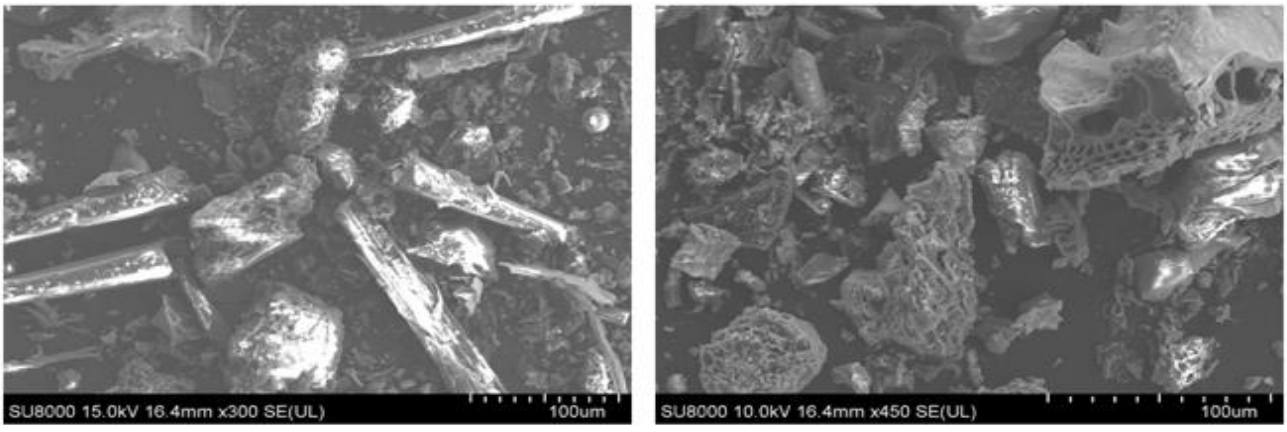

Fig. 1. SEM images of RH (a) and BC (b)

3 Results and Discussion

The morphologies of RH and BC were presented in figure 1. Typically, RH has a globular structure in nature formed by the lemma or palea, tied to each other [29,40]. The crinkle form at the epidermis is highly spiked, with conceived papillae and long-small shag on its surface [41]. Meanwhile, the morphology of the identified BC had many holes with various particle sizes, presented by the porous network and large specific surface area as listed in table 1. Table 1 showed a specific surface area of rice husk was increased after pyrolysis treatment. This finding indicates the volatilization of organics created a porous structure, resulting in a much higher surface area after further heating. The average pore size was increased too because the temperature formed a larger pore during the heating treatment process [42].

Table 1. Morphological properties of RH and BC using BET surface area analysis

Materials	Surface Area (m^2/g)	Pore Size (nm), BJH	Pore Volume $(cm^2/g)_{BJH}$
RH	7.085	3.144	0.011
BC	50.936	12.089	0.025

Fig 2 displays the powder XRD patterns of RH and BC using broad diffraction peaks. RH has two diffraction peaks denoted as (110) and (002), which were assigned as carbon and inorganic contents and used as raw starting materials. According to the results by Park *et al* [41], the (002) intense counts taken on the surface of lemma, show a dominant silica peak, which appears on the entire lemma outer surface and internal tissue of RH. The second peak indicated the formation of carbon and oxygen and their disappearance after pyrolysis. Furthermore, the pyrolysis of RH to BC, which is a carbon-rich material known as biochar remained on one peak at (002), after 3 hours. The board pattern of this material was due to the presence of amorphous silica [43]. Also, these findings are supported by increasing the surface area, pore size, and volume size as presented in table 1.

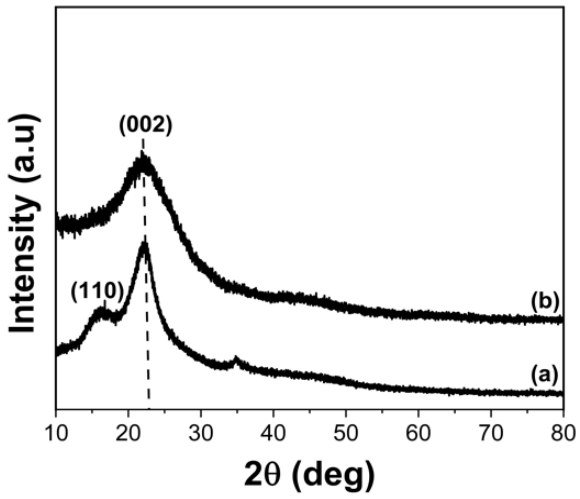

Fig. 2. XRD powder patterns of RH (a) and BC (b)

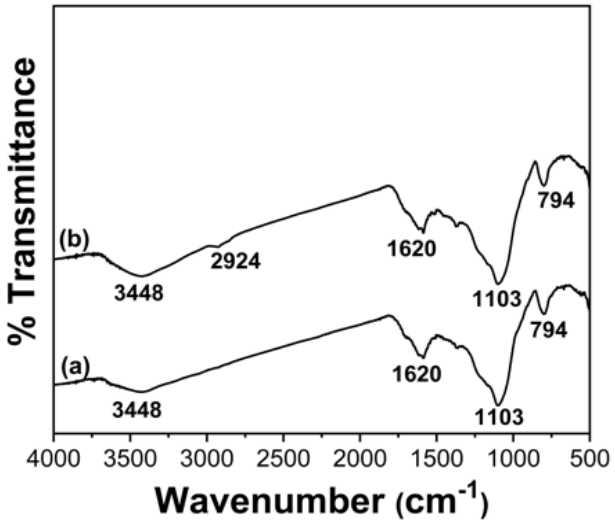

Fig. 3. FTIR spectrum of RH (a) and BC (b)

Figure 3 exhibits the FTIR images for the adsorption of RH and BC with some cases of RH peaks characteristic at 754,1103, 1620, 1800, 2924, and 3448 cm^{-1} [44,45]. The region at 3448 cm^{-1} is related to the free hydroxyl groups on the RH surface and an intensive peak at 1103 cm^{-1} denotes Si-O-Si. Meanwhile, the IR spectra indicated weak and broad peaks about 1620 cm^{-1} corresponding to the –C=O and –C–OH groups correlated with hydroxyl bonds [46]. Therefore, BC showed similar peaks with RH.

Figure 4 shows the thermograms of RH and BC with the three decomposition stages. The first was the presence of water molecule decomposition, where DTA showed the small endotherm as seen in the first peak indicating that the oxidation and this endotherm is followed by an exothermic shift. The second was the decomposition of organic compounds following the weight loss of these materials' composition. As similarly reported by Vlaev et *al* [47], the major decomposition of RH such as cellulose, lignin, and silica occurred at the temperature ranging from 500 to 650 K. Therefore, the last exothermic peaks indicated the combustion of gases product, as shown in TG which is the major weight loss of cellulose.

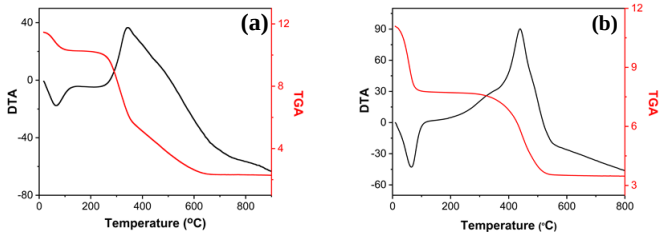

Fig. 4. TGDTA of RH (a) and BC (b)

Furthermore, RH and BC were applied as adsorbents to remove Cr (VI) in an aqueous solution. Figure 5 showed the effect of initial Cr (VI) concentration vs. adsorption capacity at various temperatures. The effect set up from 10-50 mg/g obtained a higher adsorption capacity of 16.22 mg/g and 23.01 mg/g for RH and BC, respectively at 333 K. These figures showed the increasing temperature and adsorption capacity, where equilibrium was attained in the initial concentration of 30 mg/L for RH but not for BC. However, this has not been attained at 50 mg/L, hence, the determination of the

equilibrium state from the adsorption process was described using Langmuir and Freundlich isotherm models. The formula of these models has been widely reported by other researchers [34–36,48]. Table 2 contains a list of the calculated data results.

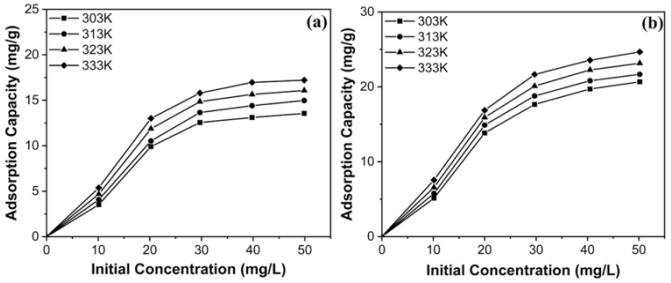

Fig. 5. Effect of initial concentration and temperature of Cr(VI) on RH and BC; adsorbent dose = 0.25 g; volume adsorbate = 0.25 L; shaking time = 120 min; pH = 3.4 ± 0.1; shaking speed = 180 rpm;

Table 2. Adsorption parameter and constant of Cr(VI) on RH and BC

Adsorbent	Adsorption Constant	T (K) 303	313	323	333
RH	Qmax	28.24	43.66	54.05	68.966
	kL	0.019	0.016	0.086	0.018
	$R^2_{Langmuir}$	0.999	0.999	0.999	0.999
	n	9.775	8.425	8.826	5.590
	kF	9.382	9.822	17.08	11.347
	$R^2_{Freundlich}$	0.999	0.999	0.999	0.989
	ΔH (kJ/mol)		9.559		
	ΔS (J/mol.K)		0.032		
	ΔG (kJ/mol)	-0.054	-0.371	-0.689	-1.006
BC	Qmax	40.65	96.15	98.03	161.29
	kL	0.060	0.015	0.037	0.006
	$R^2_{Langmuir}$	0.999	0.999	0.999	0.999
	n	6.601	9.671	7.220	10.309
	kF	13.12	12.10	14.75	11.450
	$R^2_{Freundlich}$	0.986	0.925	0.987	0.993
	ΔH (kJ/mol)		9.067		
	ΔS (J/mol.K)		0.029		
	ΔG (kJ/mol)	-0.175	-0.119	-0.412	-0.706

According to Alagha *et al* [49], Langmuir is a monolayer adsorption process, belonging to chemical sorption while Freundlich is a multilayer process that occurs with hetero-stack [19]. Based on the results in table 2, RH and BC followed Langmuir adsorption with R^2 closed to 1. The better fitting of Langmuir isotherm data means that Cr(VI) adsorption occurred in the homogeneous surface of materials. Table 2. shows BC has a higher adsorption capacity than RH at 333 K. This finding assumed that the adsorption is favored by high temperature and occupied an inactive site onto adsorbents when the saturation value was reached. Furthermore, the adsorption capacity of BC was higher than RH, due to the greater surface area and pore size of BC, as seen in table 1.

Table 3. A comparison study on the adsorption of Cr (VI) onto several adsorbents

Adsorbent	Qe (mg/g)	Ref
Plataneus orientalisleaves	5.01	[50]
Rosa damascenaphytomass	140	[51]
Rosa damascene	76	[13]
sugarcane bagasse	5.75	[15]
maize corncob	3.00	[15]
Jatropha oil cake	11.75	[15]
Coconut tree sawdust-AC	3.46	[52]
Biochar derived rice husk	4.46	[53]
Bhagalpur, Bihar, India polyaniline (PANI)	43.6	[54]
RH	68.996	Present work
BC	161.290	Present work

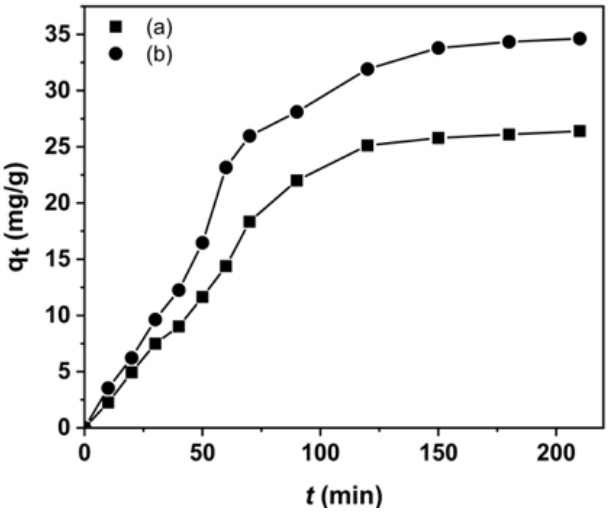

Fig. 6. Kinetic adsorption of Cr(VI) on RH (a) and BC (b); adsorbent dose = 0.25 g; volume adsorbate = 0.25 L; pH = 3.4 ± 0.1; shaking speed = 180 rpm; initial concentration = 50 mg/L; temperature condition; 303 °K.

According to previous literature, the comparison with values as listed in table 3 shows that BC is the highest in relation to the other adsorbents. These findings show BC has a high surface area and a great potential for the removal Cr (VI) from an aqueous solution.

The adsorption process was determined from the effect of time and calculated using kinetic adsorption models such as Elovich kinetic model, pseudo-1st, and -2nd orders. Also, the formula of these kinetic models has been reported by previous

researchers. Figure 6 showed the correlation between the effects of adsorption time vs. capacity. The capacity of BC was higher than RH, due to the greater surface area and pore size of BC, with both substances reaching equilibrium after 2 h. Furthermore, there was a quick increase in Cr (VI) removal initially until equilibrium reached.

Table 4 shows the adsorption kinetic model was tested by Elovich, 1st, and 2nd orders. Based on the 2nd order and Elovich data results, the adsorption data for RH and BC has R^2 all close to one, while the 1st order had R^2 >0.8. The 2nd-order model was a better fit for both RH and BC adsorbents as presented in table 4. Also, the fittings of the three models to BC were slightly better than RH, indicating the adsorption of Cr(VI) on RH was more unfavorable. These models probably described the difference between the adsorption mechanisms [55].

Table 4. Parameters of PFO, PSO, and Elovich models for RH and BC

Kinetic Models		Adsorbent	
		RH	BC
1st order	q-1st (mg/g)	43.281	76.630
	k_1 (1/min)	0.028	0.024
	R^2	0.804	0.852
2nd order	q-2nd (mg/g)	55.556	64.103
	k_2 (mg/min)	0.005	0.004
	R^2	0.967	0.983
Elovich	a (g/mg)	0.254	0.254
	b (g/mg.min)	0.106	0.083
	R^2	0.943	0.946

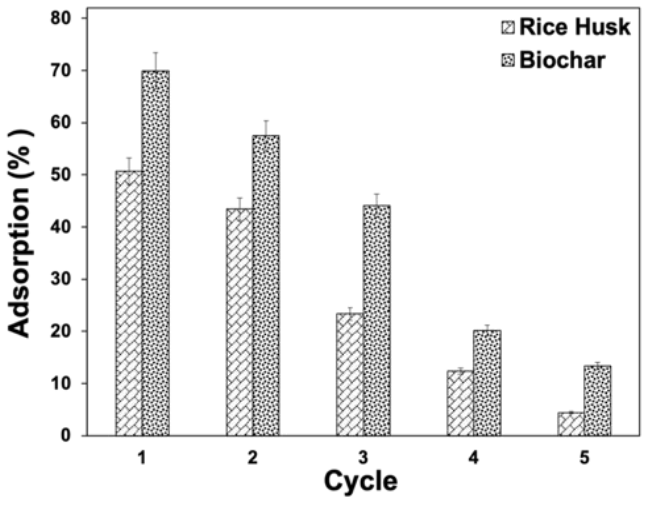

Fig. 7. Reusability of RH and BC on the adsorption of Cr(VI) ; adsorbent dose = 0.5 g; volume adsorbate = 0.25 L; shaking time = 30 min; pH = 2-4; shaking speed = 180 rpm; initial concentration = 50 mg/L; temperature condition; 303 °K.

The reusability of adsorbent was a very important study to evaluate its effectiveness. This experiment conducted five cycle adsorption-desorption treatments on RH and BC. Fig 7 shows the results of the reusability data were dramatically decreased in the fifth cycle. Also, the adsorption percentage was decreased from 69.8% to 13.4% for BC and 50.9% to 6.0% for RH. However, the efficiency of BC was better than RH assuming it has good potential as a low-cost, environment-friendly, and effective adsorbent for reuse, although BC had a low adsorption percentage after the fifth cycle.

4 Conclusion

This research showed that BC derived from Indonesian RH using thermal treatment has good proficiency in the removal of Cr(VI) from aqueous solutions. The adsorption process of this compound obtained from the adsorption capacity of biochar with a value of 161.290 mg/g at 333 K in a 2 h interaction time is comparable to RH and the other adsorbents. Furthermore, BC showed good potential as a reusable adsorbent for the removal of the heavy metal in an aqueous solution.

Acknowledgments

The authors are grateful to Universitas Sriwijaya for the financial support of this research through Hibah Profesi 2020-2021 with contract number 0687/UN9/SK.BUK.KP/2020. The authors are also grateful to the Research Center of Inorganic Materials and Complexes, Sriwijaya University for laboratory analysis and equipment.

References

1. N. Jarrah, N.D. Muazu, M. Zubair, M. Al-Harthi, *Enhanced adsorptive performance of Cr(VI) onto layered double hydroxide-bentonite composite: Isotherm, kinetic and thermodynamic studies*, Sep. Sci. Technol. 55 (2019) 1897–1909.
2. X. Zhang, L. Lv, Y. Qin, M. Xu, X. Jia, Z. Chen, *Removal of aqueous Cr(VI) by a magnetic biochar derived from Melia azedarach wood*, Bioresour. Technol. 256 (2018) 1–10.
3. T. Pavesi, J.C. Moreira, *Mechanisms and individuality in chromium toxicity in humans*, J. Appl. Toxicol. 40 (2020) 1183–1197.
4. S. Aslam, A.M. Yousafzai, *Chromium toxicity in fish: A review article*, ~ 1483 ~ J. Entomol. Zool. Stud. 5 (2017) 1483–1488.
5. D. Huang et al., *Cr(VI) removal from aqueous solution using biochar modified with Mg/Al-layered double hydroxide intercalated with ethylenediaminetetraacetic acid*, Bioresour. Technol. 276 (2019) 127–132.
6. E. Malkoc, Y. Nuhoglu, *Determination of kinetic and equilibrium parameters of the batch adsorption of Cr (VI) onto waste acorn of Quercus ithaburensis*, Chem. Eng. Process. 46 (2007) 1020–1029.
7. Y. Lu, B. Jiang, L. Fang, F. Ling, J. Gao, F. Wu, X. Zhang, *High performance NiFe layered double hydroxide for methyl*

orange dye and Cr(VI) adsorption, Chemosphere 152 (2016) 415–422.

8. F. Lyu, H. Yu, T. Hou, L. Yan, X. Zhang, B. Du, *Efficient and fast removal of Pb 2+ and Cd 2+ from an aqueous solution using a chitosan/Mg-Al-layered double hydroxide nanocomposite*, J. Colloid Interface Sci. 539 (2019) 184–193.
9. W. Qiu, Y. Zheng, *Removal of lead, copper, nickel, cobalt, and zinc from water by a cancrinite-type zeolite synthesized from fly ash*, Chem. Eng. *J*. 145 (2009) 483–488.
10. P.M.S.B.N. Siregar, N.R. Palapa, A. Wijaya, E.S. Fitri, A. Lesbani, *Structural stability of ni/al layered double hydroxide supported on graphite and biochar toward adsorption of congo red*, Sci. Technol. Indones. 6 (2021) 85–95.
11. A.S. Singha, A. Guleria, *Utility of chemically modified agricultural waste okra biomass for removal of toxic heavy metal ions from aqueous solution*, Eng. Agric. Environ. Food 8 (2015) 52–60.
12. R. Nadeem, M.N. Zafar, A. Afzal, M.A. Hanif, R. Saeed, *Potential of NaOH pretreated Mangifera indica waste biomass for the mitigation of Ni(II) and Co(II) from aqueous solutions*, J. Taiwan Inst. Chem. Eng. 45 (2014) 967–972.
13. M.J. Iqbal, F. Cecil, K. Ahmad, M. Iqbal, M. Mushtaq, M.A. Naeem, T.H. Bokhari, *Kinetic study of Cr(III) and Cr(VI) biosorption using rosa damascena phytomass: A rose waste biomass*, Asian J. Chem. 25 (2013) 2099–2103.
14. N. Kataria, V.K. Garg, *Optimization of Pb (II) and Cd (II) adsorption onto ZnO nanoflowers using central composite design: isotherms and kinetics modelling*, Elsevier B.V, (2018).
15. U. Garg, M.P. Kaur, G.K. Jawa, D. Sud, V.K. Garg, *Removal of cadmium (II) from aqueous solutions by adsorption on agricultural waste biomass*, J. Hazard. Mater. 154 (2008) 1149–1157.
16. Y. Xia et al., *Enhanced adsorption of Pb(II) onto modified hydrochar: Modeling and mechanism analysis*, Bioresour. Technol. 288 (2019) 1–8.
17. P. Gholami, L. Dinpazhoh, A. Khataee, A. Hassani, A. Bhatnagar, *Facile hydrothermal synthesis of novel Fe-Cu layered double hydroxide/biochar nanocomposite with enhanced sonocatalytic activity for degradation of cefazolin sodium*, J. Hazard. Mater. (2019) 120742.
18. E. Kulaksiz, B. Gözmen, B. Kayan, D. Kalderis, *Adsorption of Malachite Green on Fe-modified biochar: Influencing factors and process optimization*, Desalin. Water Treat. 74 (2017) 383–394.
19. A.M. Aljeboree, A.N. Alshirifi, A.F. Alkaim, *Kinetics and equilibrium study for the adsorption of textile dyes on coconut shell activated carbon*, Arab. J. Chem. 10 (2017) S3381–S3393.
20. I.M. Ríos-Badrán, I. Luzardo-Ocampo, J.F. García-Trejo, J. Santos-Cruz, C. Gutiérrez-Antonio, *Production and characterization of fuel pellets from rice husk and wheat straw*, Renew. Energy 145 (2020) 500–507.
21. S.J. Allen, G. Mckay, J.F. Porter, *Adsorption isotherm models for basic dye adsorption by peat in single and binary component systems*, J. Colloid Interface Sci. 280 (2004) 322–333.
22. B.H. Hameed, M.I. El-Khaiary, *Malachite green adsorption by rattan sawdust: Isotherm, kinetic and mechanism modeling*, J. Hazard. Mater. 159 (2008) 574–579.
23. Q. Yi et al., *Thermogravimetric analysis of co-combustion of biomass and biochar*, J. Therm. Anal. Calorim. 112 (2013) 1475–1479.
24. Y. Zhang, J. Zhao, Z. Jiang, D. Shan, Y. Lu, *Biosorption of Fe(II) and Mn(II) ions from aqueous solution by rice husk ash*, Biomed Res. Int. 2014 (2014).
25. K.Y. Foo, B.H. Hameed, *Insights into the modeling of adsorption isotherm systems*, Chem. Eng. J. 156 (2010) 2–10.
26. M.T. Tsay, F.W. Chang, *Characterization of rice husk ash-supported nickel catalysts prepared by ion exchange*, Appl. Catal. A Gen. 203 (2000) 15–22.
27. L. Leng et al., *Surface characterization of rice husk bio-char produced by liquefaction and application for cationic dye (Malachite green) adsorption*, Fuel 155 (2015) 77–85.
28. S. Chen, C. Qin, T. Wang, F. Chen, X. Li, H. Hou, M. Zhou, *Study on the adsorption of dyestuffs with different properties by sludge-rice husk biochar : Adsorption capacity , isotherm , kinetic , thermodynamics and mechanism*, J. Mol. Liq. 285 (2019) 62–74.
29. C. Sun, T. Chen, Q. Huang, J. Wang, S. Lu, J. Yan, *Enhanced adsorption for Pb(II) and Cd(II) of magnetic rice husk biochar by KMnO4 modification*, Environ. Sci. Pollut. Res. 26 (2019) 8902–8913.
30. D.V. Cuong, N.L. Liu, V.A. Nguyen, C.H. Hou, *Meso/micropore-controlled hierarchical porous carbon derived from activated biochar as a high-performance adsorbent for copper removal*, Sci. Total Environ. 692 (2019) 844–853.
31. D. Özçimen, A. Ersoy-Meriçboyu, *Removal of copper from aqueous solutions by adsorption onto chestnut shell and grapeseed activated carbons*, J. Hazard. Mater. 168 (2009) 1118–1125.
32. K.M. Poo, E.B. Son, J.S. Chang, X. Ren, Y.J. Choi, K.J. Chae, *Biochars derived from wasted marine macro-algae (Saccharina japonica and Sargassum fusiforme) and their potential for heavy metal removal in aqueous solution*, J. Environ. Manage. 206 (2018) 364–372.
33. Y. Wu, Y. Zhang, J. Qian, X. Xin, S. Hu, S. Zhang, J. Wei, *An*

exploratory study on low-concentration hexavalent chromium adsorption by Fe(III)-cross-linked chitosan beads, R. Soc. Open Sci. 4 (2017).

34. A. Lesbani, F. Asri, N.R. Palapa, T. Taher, A. Rachmat, *Efficient removal of methylene blue by adsorption using composite based Ca / Al layered double hydroxide-biochar*, Glob. NEST J. 22 (2020) 250–257.
35. W. Boulaiche, B. Hamdi, M. Trari, *Removal of heavy metals by chitin: equilibrium, kinetic and thermodynamic studies*, Appl. Water Sci. 9 (2019) 1–10.
36. L.N.H. Arakaki, V.L.S. Augusto Filha, K.S. De Sousa, F.P. Aguiar, M.G. Da Fonseca, J.G.P. Espínola, *Silica gel ethyleneimine and its adsorption capacity for divalent Pb, Cd, and Hg*, Thermochim. Acta 440 (2006) 176–180.
37. P. Saha, S. Chowdhury, S. Gupta, I. Kumar, *Insight into adsorption equilibrium, kinetics and thermodynamics of Malachite Green onto clayey soil of Indian origin*, Chem. Eng. J. 165 (2010) 874–882.
38. B.A. Fil, *Isotherm, kinetic, and thermodynamic studies on the adsorption behavior of malachite green dye onto montmorillonite clay*, Part. Sci. Technol. 34 (2016) 118–126.
39. M.R. Abukhadra, M.A. Sayed, A.M. Rabie, S.A. Ahmed, *Surface decoration of diatomite by Ni/NiO nanoparticles as hybrid composite of enhanced adsorption properties for malachite green dye and hexavalent chromium*, Colloids Surfaces A Physicochem. Eng. Asp. 577 (2019) 583–593.
40. N.T. Luyen, H.X. Linh, T.Q. Huy, *Preparation of Rice Husk Biochar-Based Magnetic Nanocomposite for Effective Removal of Crystal Violet*, J. Electron. Mater. 49 (2020) 1142–1149.
41. B.D. Park, S. Gon Wi, K. Ho Lee, A.P. Singh, T.H. Yoon, Y. Soo Kim, *Characterization of anatomical features and silica distribution in rice husk using microscopic and micro-analytical techniques*, Biomass and Bioenergy 25 (2003) 319–327.
42. K.Y. Foo, B.H. Hameed, *Utilization of rice husk ash as novel adsorbent: A judicious recycling of the colloidal agricultural waste*, Adv. Colloid Interface Sci. 152 (2009) 39–47.
43. I.J. Fernandes, D. Calheiro, A.G. Kieling, C.A.M. Moraes, T.L.A.C. Rocha, F.A. Brehm, R.C.E. Modolo, *Characterization of rice husk ash produced using different biomass combustion techniques for energy*, Fuel 165 (2016) 351–359.
44. S.M.L. Rosa, N. Rehman, M.I.G. De Miranda, S.M.B. Nachtigall, C.I.D. Bica, *Chlorine-free extraction of cellulose from rice husk and whisker isolation*, Carbohydr. Polym. 87 (2012) 1131–1138.
45. A.H. Wazir, I.U. Wazir, A.M. Wazir, *Preparation and characterization of rice husk based physical activated carbon*, *Energy Sources*, Part A Recover. Util. Environ. Eff. 00 (2020) 1–11.
46. N.R. Palapa, T. Taher, B.R. Rahayu, R. Mohadi, A. Rachmat, A. Lesbani, *CuAl LDH/Rice Husk Biochar Composite for Enhanced Adsorptive Removal of Cationic Dye from Aqueous Solution*, Bull. Chem. React. Eng. Catal. 15 (2020) 525–537.
47. L.T. Vlaev, I.G. Markovska, L.A. Lyubchev, *Non-isothermal kinetics of pyrolysis of rice husk*, Thermochim. Acta 406 (2003) 1–7.
48. M. Oktriyanti, N.R. Palapa, A. Lesbani, *Effective Removal of Iron (II) from Aqueous Solution by Adsorption using Zn / Cr Layered Double Hydroxides Intercalated with Keggin Ion*, J. Ecol. Eng. 21 (2020) 63–71.
49. O. Alagha, M.S. Manzar, M. Zubair, I. Anil, N.D. Mu'azu, A. Qureshi, *Comparative adsorptive removal of phosphate and nitrate from wastewater using biochar-MgAl LDH nanocomposites: Coexisting anions effect and mechanistic studies*, Nanomaterials 10 (2020).
50. I. Ullah, R. Nadeem, M. Iqbal, Q. Manzoor, *Biosorption of chromium onto native and immobilized sugarcane bagasse waste biomass*, Ecol. Eng. 60 (2013) 99–107.
51. M. Akram, H.N. Bhatti, M. Iqbal, S. Noreen, S. Sadaf, *Biocomposite efficiency for Cr(VI) adsorption: Kinetic, equilibrium and thermodynamics studies*, J. Environ. Chem. Eng. 5 (2017) 400–411.
52. K. Selvi, S. Pattabhi, K. Kadirvelu, *Removal of Cr(VI) from aqueous solution by adsorption onto activated carbon*, *Bioresour.* Technol. 80 (2001) 87–89.
53. A. Sarkar, A. Ranjan, B. Paul, *Synthesis, characterization and application of surface-modified biochar synthesized from rice husk, an agro-industrial waste for the removal of hexavalent chromium from drinking water at near-neutral pH*, *Clean Technol.* Environ. Policy 21 (2019) 447–462.
54. J. Ding et al., *Adsorption and Reduction of Cr(VI) Together with Cr(III) Sequestration by Polyaniline Confined in Pores of Polystyrene Beads*, Environ. Sci. Technol. 52 (2018) 12602–12611.
55. M. Inyang, B. Gao, Y. Yao, Y. Xue, A.R. Zimmerman, P. Pullammanappallil, X. Cao, *Removal of heavy metals from aqueous solution by biochars derived from anaerobically digested biomass*, Bioresour. Technol. 110 (2012) 50–56.